Proceedings of ASME Turbo Expo 2003
Power for Land, Sea, and Air
June 16–19, 2003, Atlanta, Georgia, USA

GT2003-38935

COMPARISON OF TRIP-STRIP/IMPINGEMENT/DIMPLE COOLING CONCEPTS AT HIGH REYNOLDS NUMBERS

Yong W. Kim
Leonel Arellano
Mark Vardakas
Hee-Koo Moon
Kenneth O. Smith

Solar Turbines, Inc.
San Diego, USA

ABSTRACT

Modern industrial combustor liners employ various cooling schemes such as, but not limited to, impingement arrays, trip-strips, and film cooling. With an increasing demand for a higher turbine inlet temperatures and lower emissions, there is less air available to cool the combustor liner. To ensure the required liner durability without compromising engine performance more innovative cooling schemes are required. In the present work, three different cooling concepts, i.e., strip-strips, jet array impingement and dimples, operating at unusually high flow conditions were investigated. There is very little data available in the open literature for the aforementioned cooling schemes in the indicated Reynolds Number range (Re_{Dh}>60,000). The wall flow friction characteristics as well as the local heat transfer were measured. The heat transfer coefficients were obtained using a transient liquid crystal technique. The test configurations consisted of a 90° trip-strip surface (only one side turbulated), a fixed staggered array with varying impingement hole sizes, and a fixed staggered dimple pattern. For the Reynolds numbers investigated (26,000< Re_{Dh} <360,000), the jet-impingement cooling provided the highest average heat transfer enhancement followed by the trip-strip channel, and then by the dimpled channel. In terms of the overall thermal performance, the dimpled channel tends to stand out as the most effective cooling scheme. This is consistent with findings from other investigators at lower Reynolds numbers.

NOMENCLATURE

d	concavity imprint diameter
D	impingement hole diameter
D_h	cooling channel hydraulic diameter
e	trip-strip rib height
f	fanning friction factor
g_c	proportionality constant=32.174 [lbm-ft/lbf/sec^2]
G	mass flux, ρU
h	heat transfer coefficient [Btu/hr/ft^2/^{o}F]
h_{av}	average heat transfer coefficient [Btu/hr/ft^2/^{o}F]
H	channel height
k	acrylic thermal conductivity [Btu/hr/ft/^{o}F]
k_a	air thermal conductivity [Btu/hr/ft/^{o}F]
L	length of the channel
Ma	channel average Mach number
Nu	local Nusselt number, $\frac{hD_h}{k_a}$
Nu_{av}	average Nusselt number, $\frac{h_{av}D_h}{k_a}$
Nu_o	smooth-channel Nusselt number
P	trip-strip rib spacing
Pr	Prandtl number
Re_j	jet Reynolds number, $\frac{\rho U_j D}{\mu}$
Re_{Dh}	Reynolds number, $\frac{\rho U D_h}{\mu}$
T	temperature [^{o}F]
U	mean velocity at the channel exit [ft/sec]
U_j	mean velocity through jet orifices [ft/sec]
W	width of channel
x	streamwise impingement hole spacing
y	spanwise impingement hole spacing
X_s	streamwise distance between concavities
Y_s	spanwise distance between concavities
z	jet orifice plate-to-target wall spacing

Greek

α	thermal diffusivity
Δp	pressure drop
μ	air dynamic viscosity
θ	time
ρ	air density
τ	time step

Subscripts

i	initial
m	mixed mean
s	surface

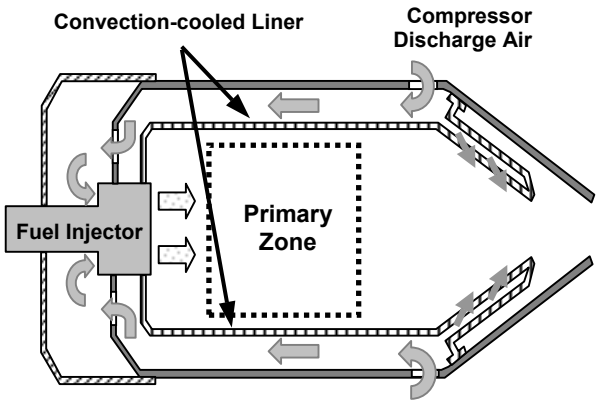

Fig.1 Serial Cooled Combustor Liner

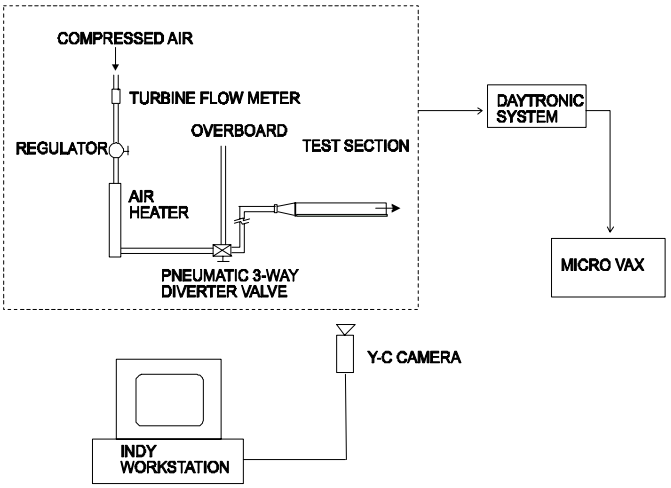

Fig.2 Schematic view of test apparatus

INTRODUCTION

Today's low-emission industrial gas turbine combustors require a creative liner cooling design that minimizes the amount of air introduced directly into the primary zone and that also allows a relatively low primary zone temperature. In this respect, a liner-cooling concept, called "serial cooling", is employed in many large engine applications. Fig.1 gives the general description of this cooling scheme. The compressor discharge air is introduced into the liner cooling passage from the downstream end side of the combustor and then routed to the fuel-injector inlet for mixing with fuel. In this scheme, the combustor liner is cooled primarily by the back-side convective heat transfer. Since the majority of compressor discharge air is routed through the fuel-injector, the back-side convection cooling passage is subject to very high flow Reynolds numbers, which are typically an order of magnitude higher than those encountered in internal cooling applications. Without reliable heat transfer and pressure loss information, the designer is forced to extrapolate from the existing correlations obtained mostly at relatively low Reynolds numbers. This has been the motivation of the present investigation where three different cooling schemes, i.e., strip-strips, jet array impingement and dimples operating at unusually high flow conditions ($26{,}000<Re_{Dh}<360{,}000$) were investigated.

Many of the early studies on heat transfer enhancement by roughened surfaces were inspired mainly by the nuclear reactor applications. The theoretical foundation of this subject was laid in the pioneering work of Nikuradse (1950) and subsequently by Dipprey and Sabersky (1963). Sheriff and Gumley (1966) presents a comprehensive experimental work which showed that heat transfer and flow friction characteristics in an annular tube with core surface roughened by wire wrapping can be successfully correlated through the existing theory. Webb et al. (1971) extended the friction and heat transfer similarity laws to correlate turbulent flow and heat transfer characteristics in tubes with periodic rib-roughness elements. Han et al. (1978) presented an experimental work on non-circular channel type configuration with partially roughened surfaces. This work covered a wide range of experimental parameters such as rib-to-channel hydraulic diameter, rib-spacing, and rib fillet angle. Many important flow and heat transfer characteristics were identified such as the optimal pitch-to-height ratio of approximately ten, and the fact that ribs with 45^o flow attack angle gave a superior thermal performance compared to that of the 90^o case. Han (1984) further modified the existing theory on rib turbulators and successfully correlated the data in convenient forms to predict the thermal performance of the rib roughened internal cooling passages of gas turbine airfoils. As the rib-roughened channels began to be used extensively in turbine blade internal cooling design, a number of experimental works emerged each with a specific emphasis (Han et al. (1985); Han (1988); Han and Park (1988)). Also, rather complex rib configurations were studied that included V-shape ribs (Lau et al. (1991) and wedge-shaped and delta-shaped roughness elements (Han et al. (1993). Bailey et al. (2002) investigated the trip-strips and impingement configurations at a high Reynolds number range ($Re_{Dh}\cong 840{,}000$) for a similar combustion application. It is noted that nearly all of the above investigations were based on test data obtained with channel Reynolds numbers less than 60,000 except Bailey et al. (2002).

Jet array impingement is widely used in gas turbine industry, especially in the cooling of hot-section static structures. Extensive studies have been reported on how the heat transfer on the target wall is impacted by jet hole diameter, hole spacing, geometrical arrangement of holes (primarily staggered and inline configurations), and target spacing. Kercher and Tabakoff (1970) and Florschuetz et al. (1980; 1981) have reported some of the most widely used heat transfer correlations used today. Bailey et al. (2002) recently reported on the impact of dense and sparse square arrays of in-line impingement jets with unidirectional flow.

Heat transfer augmentation with dimples has been known for its high thermal performance. Kesarev and Kozlov (1993) conducted a convective heat transfer test with a single concavity. Their study, which was limited to the dimple (concavity) inner region, reported that the total heat flux was about a factor of 1.5 times that of a plane circle of the same diameter at a freestream turbulence level of 0.5%. Afanasyev et al. (1993) experimentally studied the friction and heat transfer in a dimpled channel and reported a 30 to 40% heat transfer enhancement without any appreciable effect on the hydrodynamic loss. This investigation was very localized at mid-point (outside of concavity) of a staggered dimpled plate. Terekhov et al. (1995) concentrated on the surface within a concavity and concluded the existence of an optimum concavity depth.

The potential gas turbine applications of dimple designs were more recently studied by a number of investigators. Schukin et al. (1995) provided the limited data downstream of the single concavity in a diffuser channel. Chyu et al. (1997) measured a local heat transfer distribution on a surface imprinted with a staggered array of two different shapes (dimple and tear drop) of concavities. Chyu et al. (1997) also measured pressure losses and concluded that the pressure losses were nearly one-half of the protruding elements. A similar geometry was later numerically studied by Lin et al. (1999) using the low Reynolds number k-ε turbulence model. The effect of channel height on heat transfer and pressure loss was addressed by Moon et al. (2000). Through flow visualizations, Mahmood et al. (2001) showed vortical flow and vortex pairs shed from the dimples.

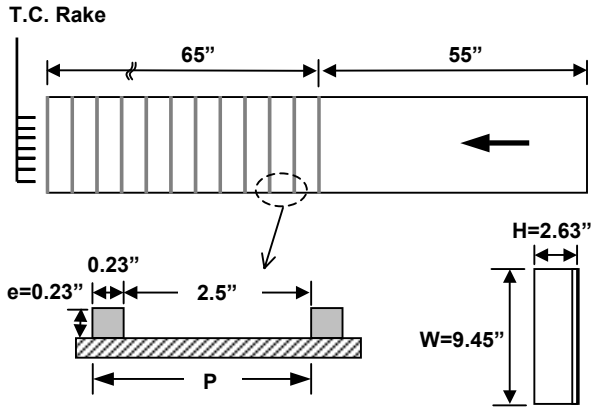

(a) Trip-Strip Channel

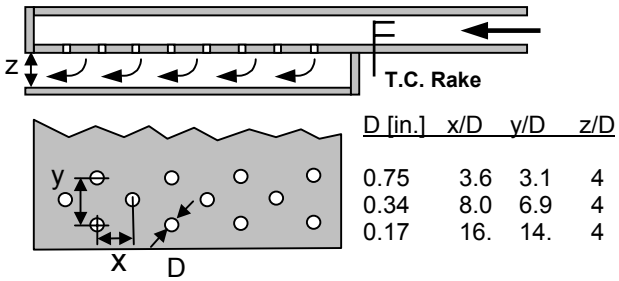

(b) Jet Array Impingement

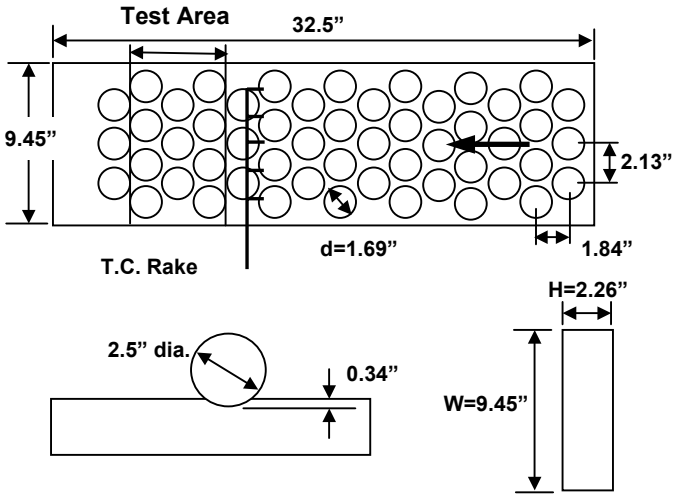

(c) Dimpled Channel

Fig.3 Test Section Geometry Detail

They also found the temperature difference (buoyancy effect) between coolant and surface enhanced heat transfer. In the present work, the flow friction characteristics as well as the local heat transfer were measured to provide a quantitative comparison between the three cooling schemes. The heat transfer coefficients were obtained using a transient liquid crystal technique. Three different test sections all made of acrylic plastic were designed to match the engine Reynolds number. The test plate configurations consisted of a 90° trip-strip surface (only one side turbulated), a fixed staggered dimple pattern, and a set of three staggered arrays of impingement holes. All of the above mentioned tests were run at a channel gap scaled from engine geometry. The friction factors and Nusselt numbers obtained from each cooling configuration were normalized by their respective fully developed smooth channel values for comparison.

TEST RIG AND DATA REDUCTION METHOD

Test Rig

Fig.2 shows a schematic of test bench used in the present investigation. Compressed air was filtered, dried, and monitored with a turbine flow meter. The plenum was equipped with a flow deflector to avert the incoming jet from the supply line reaching the channel inlet. The air was preheated to the desired temperature and diverted away from the test section until it reached steady state. The geometric details of the test section corresponding to each of the three cooling schemes studied in the present investigation are shown in Fig.3.

The test section for the trip-strip channel was a rectangular channel of 120 inches in total length with a cross-sectional dimension of 9.45” x 2.63” (height by width) as shown in Fig.3(a). The first 55 inches serve as a smooth entry length, and the remaining 65 inches form a single-wall turbulated section with equally spaced square ribs (0.23”x0.23” with a pitch of 2.73”). The impingement array test section was in the form of a rectangular plenum supplying air to the orifice plate. The plenum receives air from a channel of equal cross-sectional dimensions extending about 10 hydraulic diameters upstream. The impingement target wall was 14.2 x 21.7 inches (width by length). The impingement jet dimensions and array geometries studied are summarized in Fig.3(b). The present investigation considered only a staggered jet array pattern (8 rows) with a fixed hole spacing in both x and y directions. Different hole spacing ratios were produced by varying the jet diameter. In all three cases, the impingement distance-to-diameter ratio remained constant at z/D=4. The test surface for the dimpled channel shown in Fig.3(c) was machined to have a staggered array of concavities as shown in the figure. The test surface had a total of 15 rows of concavities. All the concavities had the same imprint diameter, depth and were equally spaced. Heat transfer coefficients were measured in the vicinity of thirteenth and fourteenth rows of concavities (indicated in the figure) to insure a fully developed thermal boundary layer. Chyu et al. (1997) took data at the downstream of the third row and claimed a thermally fully developed flow. A fixed channel height (2.3 inches) was used in the present investigation. Only one side of the channel was equipped with concavities during the entire investigation. All of the above configurations were chosen based on manufacturing constraints of a serial cooled combustor liner such as the maximum allowable channel height for the convection cooled passage. The geometric definitions for trip-strip elements and dimples were determined to produce an optimal thermal performance based on available literature data. It is noted that all three cooling concepts investigated in the present work represent a feasible design option that meets the current combustor liner durability requirement based on existing design correlations obtained at low Reynolds numbers. The test rig scale ratio (8 to 10 times the engine geometry) was determined primarily by the target nominal Reynolds number for each cooling configuration. The nominal Reynolds number varied from one configuration to anther due to the fixed available pressure drop through the cooling passage.

Data Reduction

The local heat transfer coefficient was measured with a Thermochromic Liquid Crystal (TLC) technique. The present TLC technique, which is based on a transient heat transfer solution of the semi-infinite medium suddenly exposed to a convective boundary condition, has been previously used by a number of different investigators (Ireland and Jones (1985); Vedula and Metzger (1991);

Camci et al. (1993); Yu and Chyu (1996); Ekkad et al. (1995)). The basic methodology of a transient technique was also demonstrated with use of melting paint surface coatings (Larson (1983); Larson and Metzger (1986)). The image processing system, which included a Y-C camera (Cohu 82100) and a Silicon Graphics workstation (R4000SC), digitally recorded the images of the surface pixels as they experienced a color transition during the test. The composite signal was decomposed into red, green, and blue components. The time of color change to green at each point on the test surface was the measured quantity. Green color was chosen for its signal strength and sharpness. A diffuse light-source was mounted on the camera to eliminate view-angle dependency of the TLC color transition as discussed by Herold and Wiegel (1980). Green color to temperature calibration was done on a copper coupon with TLC coating at the representative view angle at the beginning of each test. As the wall surface does not experience a pure step change in air temperature, the actual air temperature rise is represented by a superposed set of elemental steps in T_m. The fundamental solution is modified as noted by equations (1) and (2).

$$T_s - T_i = \sum_{i=1}^{N} U(\theta - \tau_i)\Delta T_m \tag{1}$$

where

$$U(\theta - \tau_i) = 1 - \exp\left[\frac{h^2\alpha(\theta - \tau_i)}{k^2}\right] erfc\left[\frac{h\sqrt{\alpha(\theta - \tau_i)}}{k}\right] \tag{2}$$

A thermal transient is initiated by using a pneumatic 3-way valve to suddenly route the heated airflow through the test section. The pneumatic 3-way valve also triggered a "time zero" light on the test section for the image processing system. In the present experiments, separate air temperature profile measurements were conducted in a transient mode. From these air temperature profile data obtained by multiple-thermocouple rake fixed at the appropriate location for each case as described in Fig3, a mixed mean air temperature (T_m) was obtained. For the trip-strips channel, the local mixed mean air temperature based on linear interpolation between inlet and exit bulk-fluid temperature was used to reduce the heat transfer results. For the dimpled channel, the local mixed mean temperature was measured at the inlet to the tested area (thirteenth row). Jet impingement results were all based on the inlet plenum total temperature.

In order to make a meaningful comparison between the three cooling schemes, an average heat transfer coefficient representative of each cooling scheme needs to be defined. A fully developed value would be a natural choice for trip-strip and dimple channels. For jet impingement, however, there is no such thing as a fully developed value. The local values are highly sensitive to the jet flow geometries such as jet spacing-to-diameter ratio and impingement distance. The three jet impingement configurations considered in the present investigation are all actual candidates for a serial cooled combustor liner in terms of number of jet rows in the streamwise direction. To this end, the area averaged heat transfer coefficient of the entire target surface was chosen to compare against the fully developed values from the other two cooling schemes. The average heat transfer coefficient was then used to calculate an average Nusselt number based on the target wall channel hydraulic diameter to compare with trip-strip and dimple channel cooling schemes. It is noted, however, the jet impingement results should be treated as three different case studies due to the variation in hole size and will be discussed accordingly. The average Nusselt number results were then normalized with the respective fully-developed turbulent flow values (Dittus and Boelter (1930)) to yield a heat transfer enhancement factor for a given Reynolds number, i.e.

$$f_N = \frac{Nu_{av}}{Nu_o} = \frac{Nu_{av}}{0.023\,\mathrm{Re}_{Dh}^{0.8}\,\mathrm{Pr}^{0.4}} \tag{3}$$

For the pressure loss experiments, one of the two side walls of each test section was instrumented with static taps in 2- to 4-inch intervals. The average friction factor was calculated from

$$f_{av} = \frac{\Delta p}{4(L/D_h)(G^2/2\rho g_c)} \tag{4}$$

In this expression, Δp is the average pressure drop across the channel for trip-strips and dimples. For jet array impingement, it was defined as the total pressure drop between plenum inlet and the last impingement row. The channel hydraulic diameter, D_h, is defined as

$$D_h = \frac{4WH}{2(W+H)} \tag{5}$$

where W and H are, respectively, the channel width and height (= z for jet impingement). G is the mass flux ($=\rho U$) through the channel cross-sectional area.

The average friction factor was normalized with the four-sided smooth duct friction factor determined from Karman-Prandtl equation modified with the aspect ratio term (Han (1984)), i.e.

$$\frac{1}{\sqrt{f_s}} = 4.0\log_{10}(\mathrm{Re}_{Dh}\sqrt{f_s}) - 0.40 + 4.0\log_{10}(r)$$

$$\text{where} \quad r = \frac{1.156 + (W/H - 1)}{W/H} \tag{6}$$

The friction enhancement factor is then defined as

$$f_F = \frac{f_{av}}{f_s} \tag{7}$$

The overall cooling performance for given pumping power can be compared using the following definition of thermal performance factor as presented in Han et al. (1985):

$$f_{PF} = f_N / f_F^{1/3} \tag{8}$$

The experimental uncertainty for the present measurement of the average Nusselt number was within $\pm$12% and was largest with the narrowest gap experiments due to their relatively high heat transfer coefficients (up to 170 Btu/hr/ft^2/^{o}F). The heat transfer level (transient time) is directly related to the experimental uncertainty, as described by Höcker (1996) who investigated the optimization of the transient TLC technique on error estimation in detail. Considering the air supply system stability and pressure transducer accuracy, the uncertainty in friction factors was estimated to be within $\pm$10%.

Uncertainties were calculated using the single sample methods of Kline and McClintock (1953) and Moffat (1988).

DISCUSSION OF RESULTS

Local Heat Transfer Distribution

The local heat transfer coefficient distributions from each of the three cases are plotted in Figs.4 through 6. Fig.4 presents a typical local heat transfer results based on the local mixed-mean air temperature in the fully developed region of the trip strips rig. The color contours show the local heat transfer trends in great details. During the initial shake-down tests, the rig went through several changes in the honeycomb flow-straightener section to reach the present level of uniformity. For the present rib orientation (90 degrees to the flow direction), no known major secondary flows exist. The local heat transfer distribution clearly shows the boundary layer reattachment occurring between the trip-strips, which is the major cause of heat transfer enhancement. Fig.5 presents the local heat transfer result for the jet array impingement obtained for the highest Reynolds number. The first four rows show a very strong stagnation behavior. The latter three rows tend to be washed out by the upstream cross-flow effects. It is believed that the tight spacing and the staggered hole pattern have contributed to the large degradation at the last two rows. Lastly, the local heat transfer coefficients obtained for the dimpled channel are plotted in a projected view of the CCD camera in Fig.6. In order to orient the relative positions of the data contours, circles representing the concavities (dimples) were overlaid on the plot. It is clear that most of heat transfer enhancement occurs outside of the concavities. The same had been previously observed in low Reynolds number cases (Re_{Dh}<55,000, Moon et al. (2000)). The heat transfer enhancement is lowest at the front portion of the concavities facing the streamwise direction, and highest at the vicinity of the downstream rim edge of the concavities.

Enhancement Factor

The average Nusselt number and friction enhancement results obtained for each cooling configuration are summarized in Figs.7 and 8. Fig.7 also shows the data from Han (1988) and Moon et al. (2000) obtained with comparable channel geometries. The trip-strip data from Han (1988), however, represent the case with trip-strips on two opposing walls as opposed to only one wall with the present rig. Han (1984) reported a 10 percent reduction in measured heat transfer between four-sided and two opposing wall ribbed ducts. Therefore, one may expect the present result be on the lower side if it were taken at lower Reynolds numbers. The present trip-strip data would suggest the rapidly decreasing enhancement factor from Han (1988) may eventually level off with increasing Reynolds number. At this point, it can be pointed out that the heat transfer enhancement factor is very comparable to the value obtained with two opposing ribbed walls at the highest Reynolds number investigated in Han (1988). The heat transfer enhancement results for three jet impingement configurations (Fig.3(b)) are plotted in three groups in Fig.7. The channel Reynolds number corresponding to each of the three distinct groups was determined by fixing the overall pressure drop for all three array configurations. Therefore, the lowest Reynolds number case represents the most sparse jet array definition used in the present investigation (D=0.166", x/D=16, y/D=14). All jet array impingement results consistently show a substantially higher enhancement factor with the exception of sparser hole pattern array at the lowest Reynolds number case (Re_{Dh}=26,200). The heat transfer enhancement factor in this case is very poor even for a sparse jet array reaching a value comparable to two opposing ribbed wall values from Han (1988). The dimple data from Moon (2000) are directly comparable to the present results with a minor difference in the channel gap height-to-concavity imprint diameter ratio (H/d=1.34 vs. 1.49). The normalized Nusselt numbers of the present study average to 2.05, compared to the 2.1 of the previous study at the

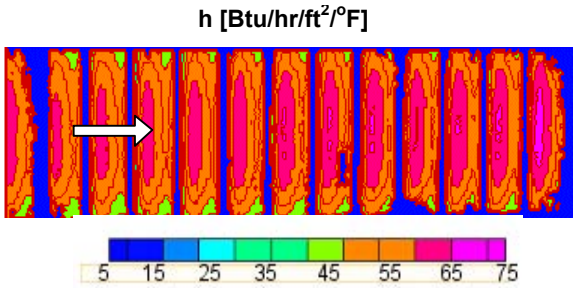

Fig.4 Trip-strip Channel: Re_{Dh}=358,000
W/H=3.6; e/D_h=0.056; P/e=11.9

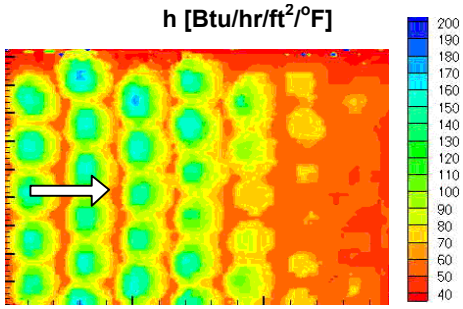

Fig.5 Jet Array Impingement
Rej= 81,280; Re_{Dh}=248,000
D=0.75"; x/D=3.6; y/D=3.1; z/D=4

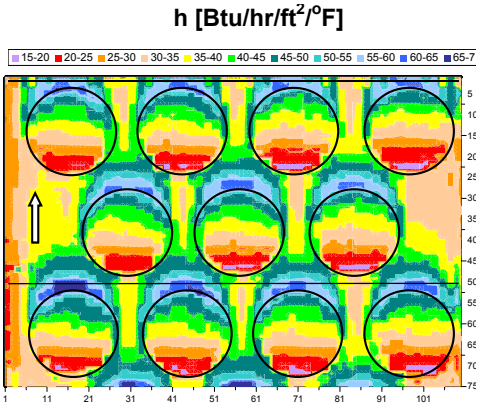

Fig.6 Dimpled Surface: Re_{Dh}=245,000
H/d=1.34; X_s/d=1.09; Y_s/d=1.26

lower Reynolds number range (30,000<Re_{Dh}<56,000, Moon et al. (2000)). The deviation (-2.4%) is therefore within the experimental uncertainty (±12%). For the dimpled channel alone, it would be fair to conclude that the aerothermal characteristics of a dimpled channel are not a strong function of Reynolds number. The friction enhancement factor results shown in Fig.8 display a large difference in magnitude showing the jet impingement case is by far the worst of all three cases in terms of pressure loss penalty. It is also of interest to observe both trip-strips and dimpled channel results display an upward trend with increasing Reynolds number in terms of pressure loss penalty, whereas the opposite is true with the jet impingement case. Dimpled channel data also show a slightly steeper slope than the trip-strips. It is noted that the present pressure-drop study for the dimpled channel was conducted at a relatively high Mach number range (0.14 <Ma<0.51), and the increasing trend of friction factor

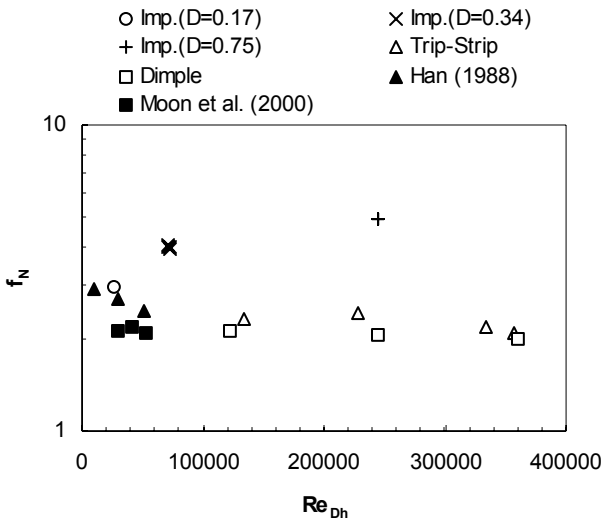

Fig.7 Nusselt Number Enhancement
Han (1988): W/H=4; e/D_h=0.078; P/e=10
Moon et al.(2000): H/d=1.49; X_s/d=1.09; Y_s/d=1.26

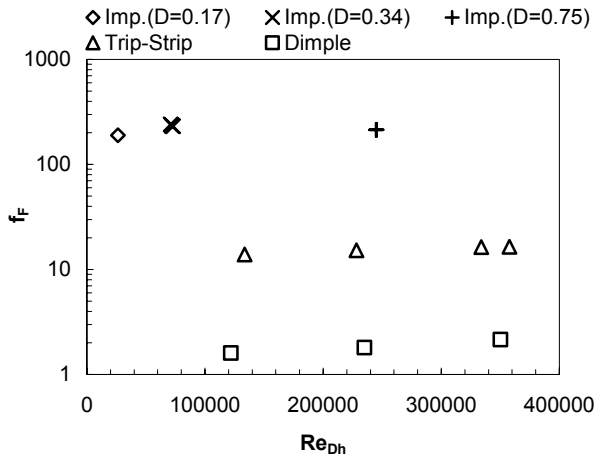

Fig.8 Friction Enhancement

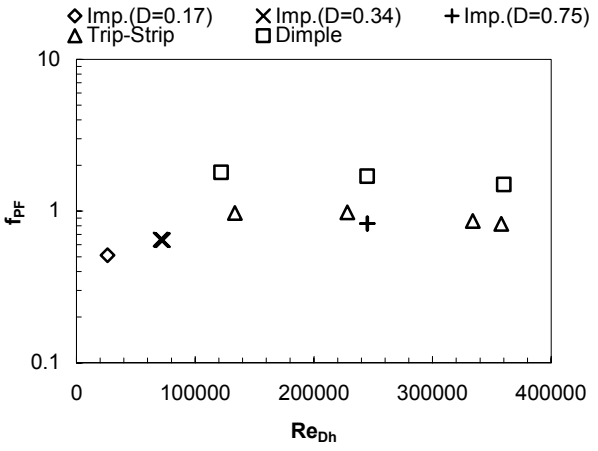

Fig.9 Overall Thermal Performance

may have been contributed to compressibility effects. Such behavior encourages one to look into the overall thermal performance factor defined as Eq.(8). Comparison of the cooling scheme performance based on this parameter will provide a quantitative assessment of the cooling performance for given pumping power or pressure drop potential. The final result based on the ratio given by Eq.(8) is plotted in Fig.9. It is noted that the dimpled surface gives the highest performance factor of the three cooling scheme for given pumping power. It is of interest to observe the trip-strip and the jet impingement results tend to display a similar thermal performance especially at high channel Reynolds numbers. This result, however, should be verified by further testing at a wider range of Reynolds numbers for each jet array configuration. It is clearly shown that the small pressure loss penalty of dimpled surface offers an advantage that makes up for the deficiency in heat transfer enhancement compared to the other two cooling schemes.

CONCLUSIONS

An experimental study has been conducted to show a quantitative comparison between three cooling schemes applicable to a serial cooled combustor liner configuration. The results of the present investigation produced the following conclusions:

1. Jet impingement provides the highest cooling, but also suffers from the largest pressure loss among the three studied cooling schemes.
2. The present trip-strip heat transfer enhancement factors are quite comparable to those of two opposing walls in the higher range of channel Reynolds numbers previously investigated.
3. The present dimple channel results display a heat transfer enhancement level similar to that of previous results obtained at much lower Reynolds numbers.
4. For given pumping power, the dimpled surface gives a superior cooling performance over jet array impingement and trip-strip surfaces.

ACKNOWLEDGEMENTS

The authors of this paper wish to thank A. French and M. Carpenter in Dept. of Development Test Engineering at Solar Turbines Inc. for their excellent craftsmanship and support leading to the completion of this project.

REFERENCES

Afanasyev, V.N., Chudnovsky, Ya.P., Leontiev, A.I., and Roganov, P.S., 1993, "Turbulent Flow Friction and Heat Transfer Characteristics for Spherical Cavities on a Flat Plate," Experimental Thermal and Fluid Science, 7:1-8, Elservier Science Publishing Co..

Bailey, J.C., Tolpadi, A.K., Intile, J., Fric, T.F., Nirmalan, N.V., and Bunker, R.S., 2002, "Experimental and Numerical Study of Heat Transfer in a Gas Turbine Combustor Liner," ASME Paper GT-2002-30183, ASME Turbo Expo 2002, Amsterdam, The Netherlands.

Camci, C., Kim, K., Hippensteele, S.A., and Poinsatte, P.E., 1993, "Evaluation of Hue Capturing Based Transient Liquid Crystal Method for High-Resolution Mapping of Convective Heat Transfer on Curved Surfaces," ASME Journal of Heat Transfer, Vol. 115, pp. 311-318.

Chyu, M.K., Yu, Y., and Ding, H., 1997, "Concavity Enhanced Heat Transfer in an Internal Cooling Passage," ASME paper 97-GT-437, International Gas Turbine and Aeroengine Congress and Exposition, Orlando, Florida.

Dipprey, D.F., and Sabersky, R.H., 1963, "Heat and Momentum Transfer in Smooth and Rough Tubes at Various Prandtl Numbers," *Int. J. Heat Mass Transfer*, Vol. 6, pp. 329-353.

Dittus, F.W., and Boelter, L.M.K., 1930, Univ. Calif. (Berkeley) Pub. Eng., Vol.2, p. 443.

Ekkad, S.V., Zapata, D., and Han J.C., 1995, "Heat Transfer Coefficients over a Flat Surface with Air and CO2 Injection Through Compound Angle Holes Using a Transient Liquid Crystal Image Method," ASME Paper 95-GT-10, 95' Turbo Expo, Houston, Texas, June 5-8.

Florschuetz, L.W., Berry, R.A., and Metzger, D.E., 1980, "Periodic Streamwise Variations of Heat Transfer Coefficients For Inline And Staggered Arrays of Circular Jets With Crossflow of Spent Air," Trans. ASME, Journal of Heat Transfer, Vol. 102, Feb., pp. 132-137.

Florschuetz, L.W., Truman, C.R., and Metzger, D.E., 1981, "Streamwise Flow and Heat Transfer Distributions For Jet Array Impingement With Crossflow," Trans. ASME, Journal of Heat Transfer, Vol. 103, May, pp. 337-342.

Han, J.C., 1984, "Heat Transfer and Friction in Channels With Two Opposite Rib-Roughened Walls," Trans. ASME, Journal of Heat Transfer, Vol. 106, Nov., pp. 774-781.

Han, J.C., 1988, "Heat Transfer and Friction Characteristics in Rectangular Channels With Rib Turbulators," Trans. ASME, Journal of Heat Transfer, Vol. 110, May, pp. 321-328.

Han, J.C., and Park, J.S., 1988, "Developing Heat Transfer in Rectangular Channels With Rib Turbulators," *Int. J. Heat Mass Transfer*, Vol. 31, No.1, pp. 183-195.

Han, J.C., and Zhang, Y.M., 1992, "High Performance Heat Transfer Ducts With Parallel Broken And V-Shaped Broken Ribs," *Int. J. Heat Mass Transfer*, Vol. 35, No. 2, pp. 513-523.

Han, J.C., Glicksman, L.R., and Rohsenow, W.M., 1978, "An Investigation of Heat Transfer And Friction For Rib-Roughened Surfaces," *Int. J. Heat Mass Transfer*, Vol. 21, pp. 1143-1156.

Han, J.C., Huang, J.J., and Lee, C.P., 1993, "Augmented Heat Transfer in Square Channels With Wedge-Shaped and Delta-Shaped Turbulence Promoters," Enhanced Heat Transfer, Vol. 1, No.1, pp. 37-52.

Han, J.C., Park, J.S., and Lei, C.K., 1985, "Heat Transfer Enhancement in Channels With Turbulence Promoters," ASME, J. Engineering For Gas Turbines and Power, Vol. 107, July, pp. 628-635.

Herold, W., and Wiegel, D., 1980, "Problems of Photographic Documentation of Liquid Crystalline Thermographs," Advances in Liquid Crystal Research and Applications," L. Bata, ed., Pergamon Press, Oxford, pp. 1255-1259.

Höcker, R., 1996, "Optimization of Transient Heat Transfer Measurements Using Thermochromic Liquid Crystals Based on Error Estimation," ASME Paper 96-GT-235.

Ireland, P.T. and Jones, T.V., 1985, "The Measurement of Local Heat Transfer Coefficients in Blade Cooling Geometries," Proceedings of AGARD Conference on Heat Transfer and Cooling in Gas Turbines, CP. 390 Paper 28, Bergen.

Kercher, D.M., and Tabakoff, W., 1970, "Heat Transfer by a Square Array of Round Air Jets Impinging Perpendicular to a Flat Surface Including The Effect of Spent Air," ASME, Journal of Engineering for Power, Jan., pp.73-82.

Kesarev, V.S., and Kozlov, A.P., 1993, "Convective Heat Transfer in Turbulized Flow Past a Hemispherical Cavity," Heat Transfer Research, Vol. 25, No. 2, Scripta Technica, Inc.

Kline, S.J., and McClintock, F.A., 1953, "Describing Uncertainties in Single Sample Experiments," Mechanical Engineering, Vol. 75, pp. 3-8.

Larson, D.E., 1983, "Transient Local Heat Transfer Measurements in 90^{o} Bends Using Surface Coatings Having Prescribed Melting Points," MS Thesis, Arizona State University.

Lau, S.C., Kukreja, R.T., and McMillin, R.D., 1991, "Effects of V-Shaped Rib Arrays on Turbulent Heat Transfer And Friction of Fully Developed Flow in a Square Channel," *Int. J. Heat Mass Transfer*, Vol. 34, No.7, pp. 1605-1616.

Lin, Y.-L., Shih, T. I-P., and Chyu, M.K., 1999, "Computations of Flow and Heat Transfer in a Channel with Rows of Hemispherical Cavities," ASME Paper 99-GT-263, Turbo Expo, Indianapolis, Indiana, June 7-10,.

Mahmood, G.I., Hill, M.L., Nelson, D.L., Ligrani, P.M., Moon, H.K., and Glezer, B., 2001, "Local Heat Transfer and Flow Structure on and Above a Dimpled Surface in a Channel," ASME, J. of Turbomachinery, Vol. 123, pp. 115-123.

Metzger, D.E., and Larson, D.E., 1986, "Use of Melting Point Surface Coatings for Local Convection Heat Transfer Measurements in Rectangular Channel Flows With 90-deg Turns," ASME, Journal of Heat Transfer, Vol. 108, pp. 48-54.

Moffat, R.J., 1988, "Describing the Uncertainties in Experimental Results, Experimental Thermal and Fluid Sciences, Vol. 1, pp. 3-17.

Moon, H.K., O'Connell, T., and Glezer, B., 2000, "Channel Height Effect on Heat Transfer and Friction in a Dimpled Passage," ASME, J. of Engineering for Turbines and Power, Vol. 122, pp.307-313.

Nikuradse, J., 1950, "Laws of Flow in Rough Pipes," VDI Forsch, 361 (1933), English Translation: NACA TM-1292

Rohsenow, W.M., and Hartnett, J.P., 1973, Handbook of Heat Transfer, McGraw-Hill, New York, pp. 7-122.

Schukin, A.V., Kozlov, A.P., and Agachev, R.S., 1995, "Study and Application of Hemispherical Cavities for Surface Heat Transfer Augmentation," ASME paper 95-GT-59, International Gas Turbine and Aeroengine Congress and Exposition, Houston, Texas.

Sheriff, N., and Gumley, P., 1966, "Heat-Transfer And Friction Properties of Surfaces With Discrete Roughnesses," *Int. J. Heat Mass Transfer*, Vol. 9, pp. 1297-1320.

Terekhov, V.I., Kalinina, S.V., and Mshvidobadze, Y.M., 1995, "Flow Structure and Heat Transfer on a Surface with a Unit Hole Depression," Russian J. of Engineering Thermophysics, Vol. 5, pp. 11-34.

Vedula, R.J., and Metzger, D.E., 1991, "A Method for the Simultaneous Determination of Local Effectiveness and Heat Transfer Distributions in Three Temperature Convection Situations," ASME Paper 91-GT-345.

Webb, R.L., Eckert, E.R.G., and Goldstein, R.J., 1971, "Heat Transfer And Friction in Tubes With Repeated-rib Roughness," *Int. J. Heat Mass Transfer*, Vol. 14, pp. 601-617.

Yu, Y., and Chyu, M.K., 1996, "Influence of a Leaking Gap Downstream of the Injection Holes on Film Cooling Performance," ASME Paper 96-GT-175, ASME Turbo Expo '96, Birmingham, UK, June 10-13.